Hydrogen adsorption, dissociation and diffusion on the α-U(001) surface

2008 J. Phys.: Condens. Matter 20 445001

(http://iopscience.iop.org/0953-8984/20/44/445001)

J. Phys.: Condens. Matter **20** (2008) 445001 (10pp) doi:10.1088/0953-8984/20/44/445001

Hydrogen adsorption, dissociation and diffusion on the α-U(001) surface

J L Nie[1], H Y Xiao[1], X T Zu[1,3] and Fei Gao[2]

[1] Department of Applied Physics, University of Electronic Science and Technology of China, Chengdu 610054, People's Republic of China
[2] Pacific Northwest National Laboratory, MS K8-93, PO Box 999, Richland, WA 99352, USA

E-mail: xiaotaozu@yahoo.com

Received 22 May 2008, in final form 23 July 2008
Published 12 September 2008
Online at stacks.iop.org/JPhysCM/20/445001

Abstract

First-principles pseudopotential plane-wave calculations based on density functional theory and the generalized-gradient approximation have been used to study the adsorption, dissociation, and diffusion of hydrogen on the α-U(001) surface. Weak molecular chemisorption was observed for H_2 approaching with its molecular axis parallel to the surface. The optimization of the adsorption geometries on the threefold hollow sites yields final configurations with H_2 molecules moving towards the top site at both coverages considered, 0.25 and 0.5 monolayers. A low dissociation barrier of 0.081 eV was determined for H_2 dissociated from the onefold top site with the H atoms falling into the two adjacent threefold hollow sites. The analysis of the density of states along the dissociation paths shows that the hybridization of U 5f and H 1s states only occurs when the H_2 molecule is dissociated.

(Some figures in this article are in colour only in the electronic version)

1. Introduction

Uranium (U) hydriding is one of the most important processes in surface corrosion, which has received considerable attention for over sixty years [1–7]. The study on the U–H system is not only of fundamental interest but also technologically important in the nuclear industry, due to its environment corrosion process and hydrogen storage potential. In the past few decades, many works have been addressed to the thermochemistry, diffusion kinetics and hydriding mechanisms of U–H systems. An early experimental work performed by Condon and Larson focused on the reaction kinetics of $U + \frac{3}{2}H_2 \leftrightarrow UH3$ with a reaction mechanism proposed for the U hydriding process [4]. Also Condon calculated and measured the reaction rates of U hydriding and proposed a diffusion model for the U hydriding which was found to be in excellent agreement with the experimental reaction rates [3]. The kinetics and mechanism for the U–H reaction over a wide range of pressures and temperatures have been studied by Bloch and Mintz who have obtained two-dimensional fits of experimental data to the pressure–temperature reactions [2]. The study of U hydriding in ultrahigh vacuum by Powell *et al* gave linear rate data over a wide range of temperatures and pressures [7].

Due to the high reactivity of U with environmental gases, surface corrosion is critical in nuclear applications. As the initial stage in the surface corrosion process, chemisorption of gases to solid surfaces plays an important role in surface corrosion. In recent years, advances in theoretical and computational formalisms have significantly increased research into strongly correlated materials and heavy fermion systems. The chemisorption of carbon monoxide [8] and oxygen gas [9] on the γ-U surface has been investigated using the density functional semicore pseudopotential method focusing on the geometric, magnetic and electronic properties of the system. Senanayake *et al* have studied carbon monoxide adsorption on α-U surfaces using a plane-wave ultrasoft pseudopotential [10]. For the U–H system, although the above review has shown that studies of thermochemistry, diffusion kinetics and hydriding mechanisms are abundant, a systematic adsorption study on the surface is still lacking. The current study mainly focused on the chemisorption, dissociation and diffusion of hydrogen on the (001) surface of α-U, providing important insights into the mechanism of the U hydrogenation process.

[3] Author to whom any correspondence should be addressed.

2. Computational details

The calculations performed in this study were done using the *ab initio* total-energy and molecular dynamics program VASP (Vienna *ab initio* simulation program) [11]. This program evaluates the total energy of periodically repeating geometries on the basis of density functional theory (DFT) and the pseudopotential approximation. The interaction between ions and electrons is described using the projector augmented wave (PAW) method [12, 13]. The generalized-gradient approximation (GGA) of Perdew and Wang known as PW91 was employed for the exchange–correlation functional in the calculations [14]. A plane-wave basis set was used to expand the electronic wavefunctions with a plane-wave energy cutoff of 350 eV, which leads to an absolute error in the total energy of less than 2 meV/atom. All energies are extrapolated to $T = 0$ K. The minimization of the electronic free energy is carried out using an efficient iterative matrix-diagonalization routine based on a sequential band-by-band residuum minimization method (RMM). Monkhorst–Pack k points were used to sample the Brillouin zone. A smearing function of the Methfessel–Paxton (MP) type (a product of a Gaussian times an nth-order Hermite polynomial) was used throughout. To determine the degree of convergence with respect to the number of k points, a series of calculations were performed. The k-point grid of $7 \times 7 \times 1$ (consisting of a total of 25 k points in the irreducible Brillouin zone) generally gives a well converged result in the surface calculations. The validity of the U pseudopotential has been tested, with good agreement obtained between the calculated bulk properties and the experimental values as presented in our previous work [15]. In view of the quick convergence of the surface energy of α-U(001) [15] and the computational efficiency, a three-layer slab of α-U(001), periodically repeated in a supercell geometry with 10 Å of vacuum between any two successive metal slabs, was used to model the adsorbate–substrate system. Single-sided adsorption was used in all of the adsorption structure calculations. All of the substrate atoms and the hydrogen adsorbates were allowed to relax.

The climbing-image nudged elastic band (CNEB) method was used to determine the minimum energy paths for H_2 dissociation and atomic H diffusion. CNEB is an improved version of the original NEB method. It allows the image with the highest energy to climb to the saddle point, which therefore permits an accurate determination of the transition state. This image does not feel the spring forces along the band. Instead, the true force for this image along the tangent is inverted. In this way, the image 'tries' to maximize its energy along the band, and minimize it in all other directions. When this image converges, it will be at the exact saddle point. For a detailed technical explanation of the NEB method, see [16–19].

3. Results and discussion

The adsorption of H_2 on the α-U(001) surface has been calculated using 2×1 and 1×1 cells. One H_2 molecule was put on both cells, corresponding to the coverages of 0.25 and 0.5 monolayers (ML). Five possible symmetrically distinguishable on-surface sites (see figure 1), denoted as hollow1, hollow2, long-bridge, short-bridge and top, have been considered. For each of these sites, three configurations were taken into account as illustrated in figure 2. They are: (a) the H_2 molecule adsorbs perpendicular to the surface (denoted as 'Ver'), (b) the H_2 molecule adsorbs parallel to the surface and one of the lattice vectors (denoted as 'Hor1'), and (c) the H_2 molecule adsorbs parallel to the surface and another surface lattice vector (denoted as 'Hor2').

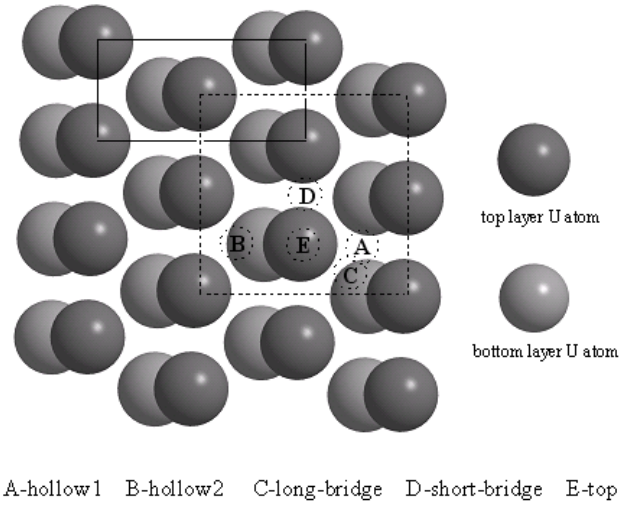

Figure 1. Schematic illustration of the surface cells and adsorption sites. The solid and dashed cells correspond to (1×1) and (2×1), respectively.

For all configurations the corresponding adsorption energies were calculated according to the expression

$$E_{\text{ads}} = E_{\text{slab}} + E_{\text{H}_2} - E_{\text{H}_2+\text{slab}} \tag{1}$$

where $E_{\text{H}_2+\text{slab}}$ is the total energy of the optimized adsorbate/slab system, E_{slab} is the total energy of the relaxed slab, and E_{H_2} is the energy of the optimized isolated H_2 molecule. A positive adsorption energy corresponds to a stable adsorbate/slab system. Table 1 contains the optimized adsorption parameters and adsorption energies. For the case of tilted H_2, the tilt angle is defined as the angle formed by the H–H bond and a vector drawn normal to the surface. The energy of adsorption onto the surface of a molecule is given in the column labeled 'E_{ads}' in units of eV. All other entries are defined in the footnotes to the table.

H_2 molecules adsorbed in Ver configurations rotate slightly in a plane perpendicular to the U surface upon optimizing, leading to titled final configurations at an angle between $\sim 2°$ and $\sim 30°$ relative to the surface normal. The adsorption energies of Ver configurations are very small, up to 53 meV at $\Theta = 0.25$ ML and 27 meV at $\Theta = 0.5$ ML, indicating that the H_2 molecule physisorbs onto the surface when it approaches with its molecular axis perpendicular to the surface. This is consistent with H_2 adsorption on the heavy metal surface of Pu(111) [20].

At the coverage of 0.25 ML, both horizontal configurations on the long-bridge site and the Hor1 configuration on the

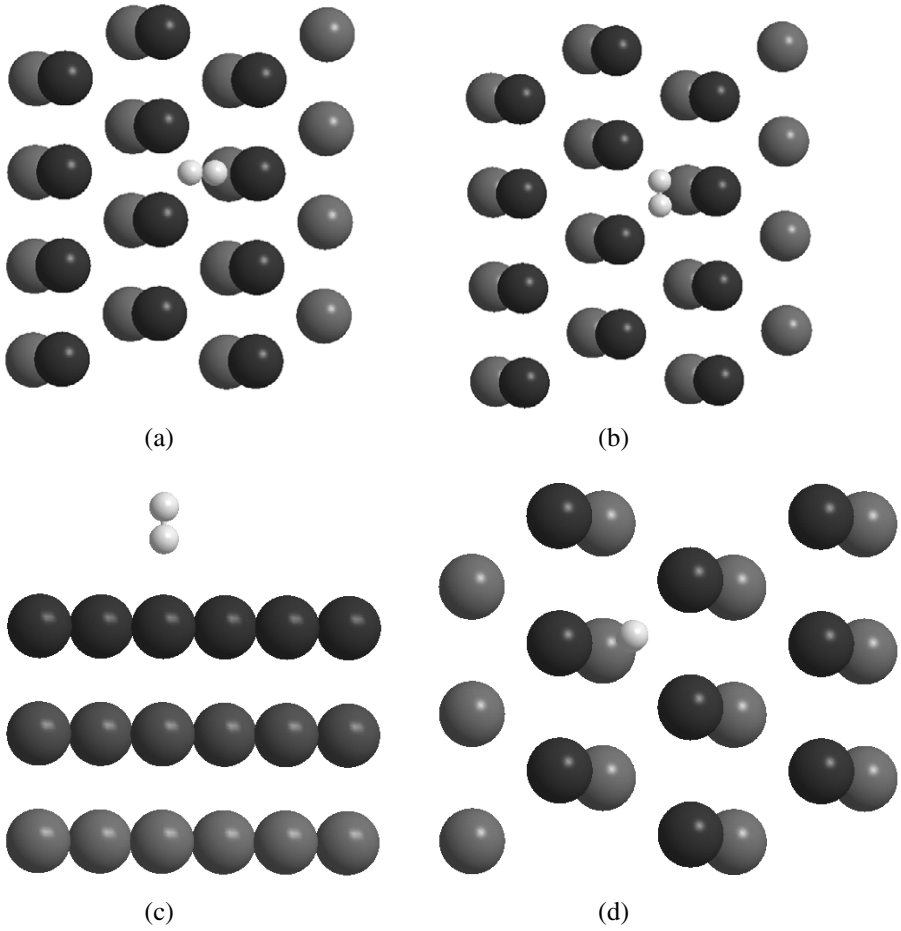

Figure 2. Horizontal and vertical adsorption configurations for H_2 on the threefold hollow2 site: (a) top view of the Hor1 configuration, (b) top view of the Hor2 configuration, (c) side view of the Ver configuration, (d) top view of the Ver configuration. The small white spheres correspond to the hydrogen atoms and the dark ones represent the uranium atoms.

short-bridge site are found to be unstable for H_2 adsorption. On the other hand, an H_2 molecule physisorbs onto the surface at Hor2 on the short-bridge site in a low adsorption energy of 0.041 eV. H_2 adsorption onto the onefold top site is stable at Hor1 and Hor2 at adsorption energies of 0.213 and 0.309 eV, respectively. All horizontal adsorption configurations on both hollow sites are found to considerably change in geometry upon optimizing. The optimized Hor1 configuration on the hollow1 site has the highest energy, which is only an 8 meV preference over Hor2. For the Hor1 configuration, a significant rotation (90°) parallel to the surface, together with considerable lateral shift of the center of the H_2 molecule, was found, which leads to a final configuration similar to Hor2 on the top site (not exactly on the top site). For the Hor2 configuration, the adsorbed H_2 molecule also moves towards the top site. The horizontal configurations on the hollow2 site behave very similarly to those on the hollow1 site. Huda and Ray have also reported that H_2 molecules adsorbed on Pu(111) surfaces onto center sites move towards the top site [20]. The tilt angles of the H_2 molecule were found by examination to be ∼90° relative to the surface normal, indicating that H_2 adsorbs almost parallel to the surface.

As the coverage increases to 0.5 ML, H_2 molecules adsorbed at both horizontal configurations on the hollow sites were found to move towards the top site. It is interesting to find that the rotation parallel to the surface for H_2 molecules at Hor1 on hollow sites which was observed at $\Theta = 0.25$ ML did not present at the coverage of 0.5 ML. This may be attributed to the increasing lateral H_2–H_2 repulsive interactions. The adsorption on the twofold bridge sites is found to be unstable. The calculated energetic results show that the Hor2 configuration on the hollow2 site (close to the top site) is lowest in energy; this is nearly degenerate with Hor2 configurations on the top and the optimized hollow1 sites. It is noted that the adsorption energy of H_2 at $\Theta = 0.5$ ML is somewhat lower than that at $\Theta = 0.25$ ML, indicating weaker adsorption with increasing coverage. This is consistent with the previously reported TPD result, indicating that the desorption peak of H_2 on the U surface shifts to lower temperature with increasing coverage [21]. It is indicated that an H_2 molecule at Hor1 on both hollow sites is somewhat tilted, with an angle of ∼70° relative to the surface normal.

The calculated adsorption geometric parameters show that the interatomic distance R(U–H) is about 2.3 Å for various stable Hor configurations. For the Ver configurations, R(U–H) is stretched to 3.2–3.8 Å for the H atoms, which is indicative of a weak physisorption. The H–H bond lengths are slightly elongated for all stable adsorption configurations relative to

Table 1. Calculated equilibrium distances and adsorption energies for the H_2 molecule adsorbed on the α-U(001) surface at different sites and for different coverages. (Note: E_{ads} denotes the adsorption energy. R(H–U) represents the shortest binding length between the adsorbed H and surface U atoms. h(H–Surf) is the average binding height with respect to the first layer Z. φ represents the angle between the H–H bond and the normal to the surface. $\Delta Z_{12}/d_0$ and $\Delta Z_{23}/d_0$ represent the relaxation of the first and second interlayer spacings of the U slab with respect to the bulk value d_0. The two columns for R(H–U) and h(H–Surf) correspond to the two H atoms of H_2.)

Configuration		E_{ads} (eV)	R(H–H) (Å)	R(H–U) (Å)		h(H–Surf) (Å)		φ (deg)	$\Delta Z_{12}/d_0$ (%)	$\Delta Z_{23}/d_0$ (%)
U(2 × 1)–H_2										
Hollow1	Hor1	0.370	0.841	2.260	2.277	2.148	2.135	89.1	−3.4	−3.7
	Hor2	0.362	0.861	2.238	2.250	2.058	2.033	88.4	−3.5	−3.7
	Ver	0.046	0.769	3.165	2.760	2.914	2.239	28.8	−3.8	−3.9
Hollow2	Hor1	0.337	0.819	2.306	2.290	2.237	2.263	88.2	−3.4	−3.8
	Hor2	0.276	0.821	2.331	2.339	2.282	2.236	86.7	−3.3	−3.8
	Ver	0.021	0.774	3.205	2.804	2.970	2.298	29.8	−3.7	−3.9
Lbri	Ver	0.041	0.772	3.466	2.855	3.082	2.336	14.8	−3.7	−3.8
Sbri	Hor2	0.041	0.751	3.506	3.512	3.324	3.336	89.1	−3.8	−3.8
	Ver	−0.009	0.778	3.270	2.602	2.914	2.137	1.70	−3.7	−3.8
Top	Hor1	0.213	0.794	2.375	2.378	2.328	2.318	89.3	−3.5	−3.9
	Hor2	0.309	0.822	2.275	2.276	2.231	2.231	89.9	−3.6	−3.9
	Ver	0.053	0.750	3.751	3.017	3.746	3.011	11.9	−3.9	−3.8
U(1 × 1)–H_2										
Hollow1	Hor1	0.186	0.806	2.398	2.374	2.357	2.088	70.5	−3.5	−3.9
	Hor2	0.254	0.812	2.329	2.329	2.232	2.232	90.0	−3.8	−3.9
	Ver	0.006	0.770	3.248	2.747	2.977	2.256	20.5	−4.2	−4.2
Hollow2	Hor1	0.184	0.790	2.385	2.454	2.255	2.448	75.8	−3.4	−3.9
	Hor2	0.264	0.821	2.345	2.345	2.311	2.311	90.0	−3.5	−4.1
	Ver	0.014	0.769	3.297	2.864	3.088	2.415	28.9	−4.0	−4.0
Lbri	Ver	0.007	0.767	3.570	2.922	3.202	2.443	8.40	−4.0	−4.3
Sbri	Hor2	−0.002	0.749	3.886	3.634	3.453	3.481	87.8	−4.4	−4.0
	Ver	0.027	0.759	3.853	3.183	3.580	2.847	15.1	−4.1	−3.8
Top	Hor1	0.209	0.789	2.385	2.394	2.339	2.325	88.9	−3.5	−4.0
	Hor2	0.263	0.815	2.309	2.309	2.264	2.264	90.0	−3.7	−4.2
	Ver	0.027	0.754	3.593	2.882	3.585	2.873	19.1	−4.1	−4.1

the optimized isolated gas phase equilibrium distance of H_2 (0.748 Å). The surface relaxation due to H_2 adsorption has also been summarized in table 1, which shows that the spacing between the top two layers (Δd_{12}) decreases by −3.0 to −4.0% relative to the bulk interlayer spacing, and the distance between the next two layers (Δd_{23}) also shows a decrease of similar magnitude. This indicates that a surface contraction occurs due to the adsorption of H_2.

In addition to the H_2 molecular adsorption, we have studied the adsorption of individual H atoms on α-U(001). To investigate the atomic adsorption behavior at various coverages, two adsorption patterns, α-U(001) (2 × 1)–H and α-U(001) (1 × 1)–H, corresponding to the coverages of 0.25 and 0.5 ML, have been considered. All highly symmetric sites as described previously have been taken into account. Two subsurface positions sub1 (directly below the hollow1 site) and sub2 (directly below the hollow2 site) have also considered, by moving the hollow hydrogen overlayer below the top metal layer.

The adsorption energies of hydrogen atoms were estimated following the formula

$$E_{ads} = (E_{slab} + E_H - E_{H+slab})/n \quad (2)$$

where E_{H+slab} is the total energy of the adsorption configuration. n denotes the number of hydrogen atoms and E_H represents the energy of the isolated hydrogen atom calculated with spin polarization.

At both coverages, H atoms adsorbed on the hollow sites are found to finally move by ∼0.4 Å towards the short-bridge site upon optimizing. The long-bridge site is unstable at $\Theta = 0.25$ ML and becomes stable as the coverage increases to 0.5 ML. The low coordination sites of top and short-bridge sites are unstable, with the H adsorbates finally occupying positions similar to those on the hollow sites. The calculated adsorption energies as listed in table 2 show that the adsorptions at the hollow2 site with adsorption energies of 2.871 eV at $\Theta = 0.25$ ML and 2.800 eV at $\Theta = 0.5$ ML are the most energetically favored. The adsorption energy for the next stable site hollow1 was determined as 2.846 eV at 0.25 ML and 2.734 eV at 0.5 ML. The long-bridge site, which is stable at 0.5 ML, is found to ∼0.2 eV higher in adsorption energy than the hollow2 site. The U–H bond lengths are 2.2 Å and the binding height of the adsorbed H atoms with respect to the surface Z was determined as 1.3–1.4 Å. A contraction of the surface upon H adsorption has also been observed at a similar magnitude to those for molecular adsorption. The adsorption at the subsurface sites was found to be considerably lower in adsorption energy than that at the on-surface adsorption sites. The subsurface adsorption of the molecule H_2 has also been investigated and found to be unstable, indicating that hydrogen does not 'prefer' to penetrate into the uranium surface. This

Table 2. Energetic and structural parameters for atomic H adsorbed on the α-U(001) surface. The label of '$h1 + h2$' represents the configuration with two hydrogen atoms occupying hollow1 and hollow2 sites, respectively.

	E_{ads} (eV)	R(H–U) (Å)	h(H–Surf) (Å)	$\Delta Z_{12}/d_0$ (%)	$\Delta Z_{23}/d_0$ (%)
			0.25 ML		
Hollow1	2.846	2.274	1.237	−3.2	−3.6
Hollow2	2.871	2.255	1.324	−3.4	−3.6
Sub1	2.100	2.082	−0.805	−0.5	−4.4
Sub2	2.169	2.049	−0.474	−1.21	−4.3
			0.5 ML		
Hollow1	2.734	2.278	1.355	−3.4	−3.4
Hollow2	2.800	2.236	1.401	−3.3	−3.5
Lbri	2.604	2.168	1.471	−3.4	−3.9
Sub1	2.018	2.111	−0.873	5.4	−5.5
Sub2	2.034	2.042	−0.551	3.2	−5.2
			1 ML		
$h1 + h2$	2.755	2.221	1.361	−2.9	−3.4
		2.226	1.341		

will also be demonstrated in the subsequent discussion of the atomic H diffusion process.

To investigate the relative thermodynamic stability of the two adsorption phases which share different stoichiometries due to the different concentrations of H, one can examine the surface formation energy of each system [22].

The formation energies [23] per (1×1) unit cell at 0 K for a slab can be written as

$$\Omega = E_{\mathrm{H/U(001)}} - n_{\mathrm{U}}\mu_{\mathrm{U}} - n_{\mathrm{H}}\mu_{\mathrm{H}} \tag{3}$$

where μ_{U} and μ_{H} are the chemical potentials of U and H, respectively. $E_{\mathrm{H/U(001)}}$ is the total energy of the adsorption system as obtained from the self-consistent *ab initio* calculations. Since the H atoms at the surface must be in equilibrium with the bulk, μ_{U} must equal $\mu_{\mathrm{U}}^{\mathrm{bulk}}$. The bulk chemical potential of U has been calculated using the same calculation procedure as for the surface calculations and the technical details are similar. μ_{H} for the gaseous hydrogen varies with pressure and temperature. We measured the hydrogen chemical potential relative to the calculated energy of the H_2 molecule, i.e.,

$$\mu_{\mathrm{H}} = \tfrac{1}{2}E(\mathrm{H_2}). \tag{4}$$

Thus $\mu_{\mathrm{H}} = 0.0$ represents the chemical potential at which an H_2 molecule can be formed with no cost in energy. The calculated formation energies as a function of μ_{H} are presented in figure 3(a).

It is shown that the range of stability for different phases varies with the relative hydrogen chemical potential. For -0.68 eV (i.e. in the H poor limit) the clean α-U(001) surface has a lower formation energy than with any amount of H adsorbed on it. For -0.68 eV $< \mu_{\mathrm{H}} < -0.44$ eV the 0.25 ML coverage adsorption is found to be the most stable structure, rather than the one with the higher coverage of 0.5 ML. The adsorption of H_2 at $\Theta = 0.5$ ML, having the least formation energy, is reached for $\mu_{\mathrm{H}} > -0.43$ eV, indicating that in the H rich limit half-coverage adsorption is possible. This result

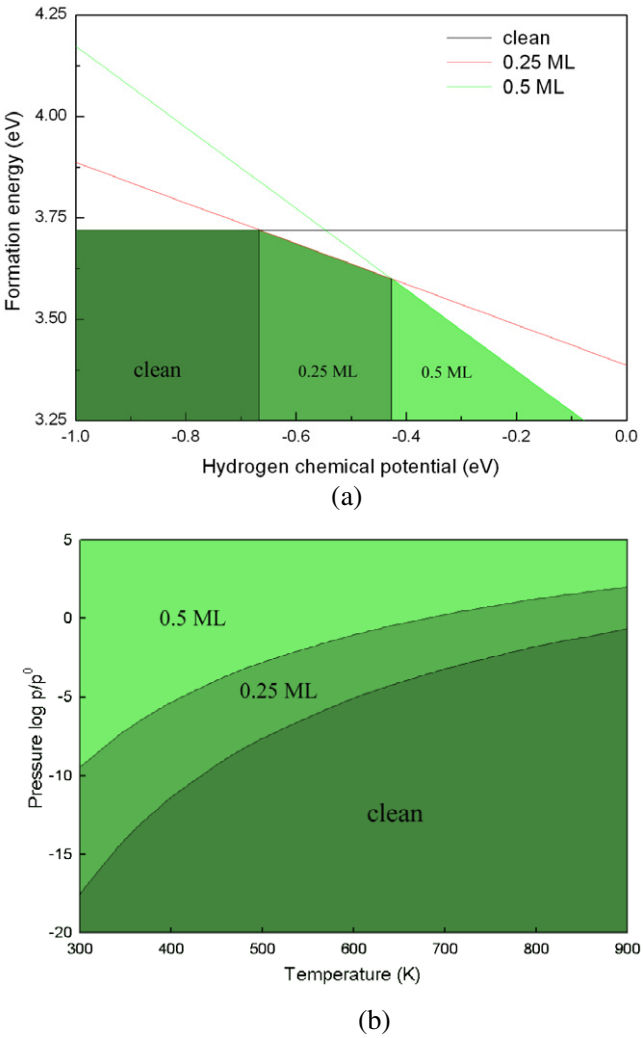

Figure 3. (a) The surface free energy of different monolayers of atomic H on α-U(001) plotted against the H chemical potential. (b) The stability range of the phases considered, evaluated in (a), plotted in the (p, T) space. The phases are distinguished by varying shades, with the phase of $\Theta = 0.5$ ML more favorable at high pressure for all temperatures considered.

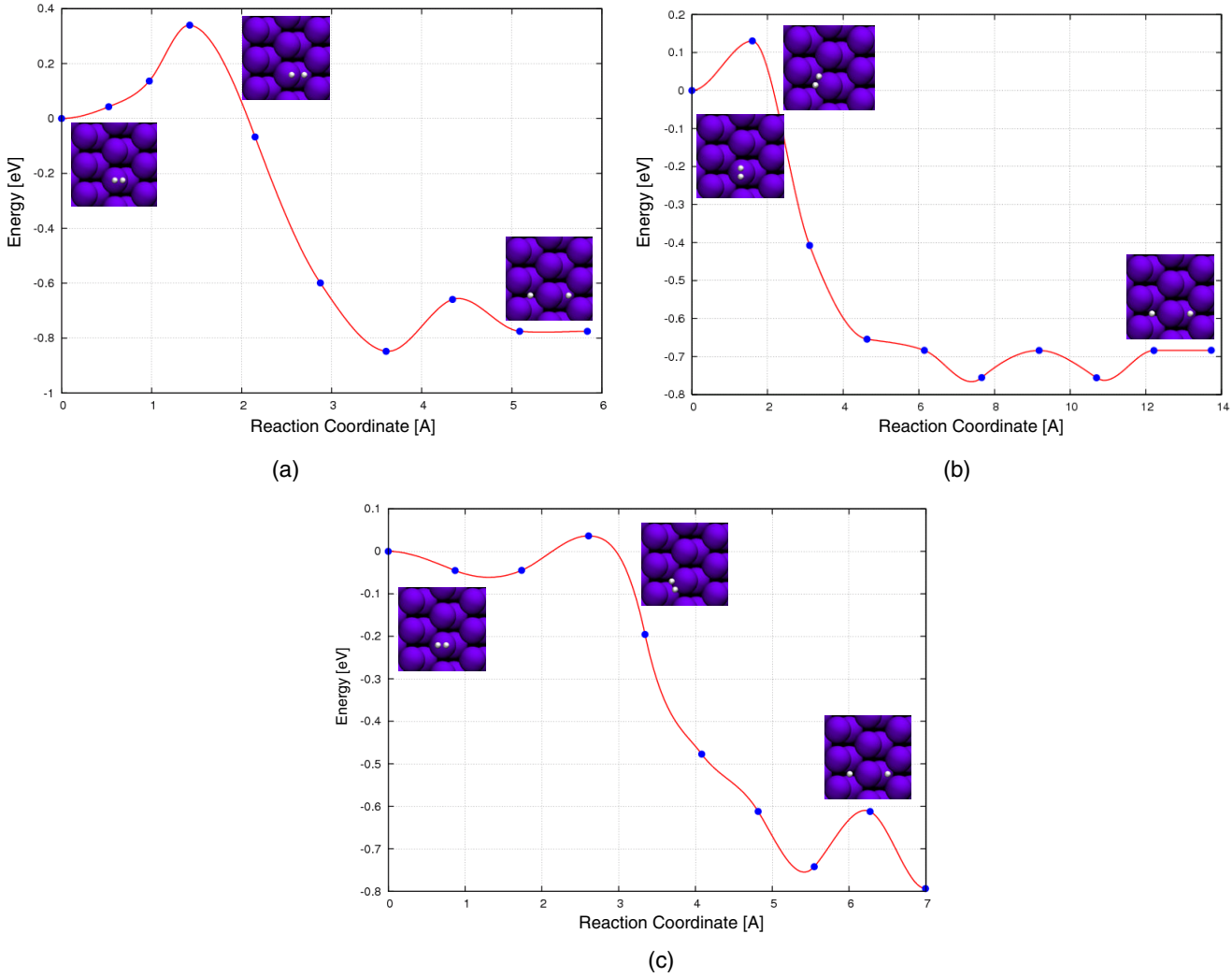

Figure 4. Potential energy surface for dissociation of an H_2 molecule at (a) the Hor1 configuration on the threefold hollow2 site, (b) the Hor2 configuration on the threefold hollow2 site and (c) the Hor1 configuration on the onefold top site. The inset structures (the small white spheres correspond to the hydrogen atoms and the large violet ones represent the uranium atoms) represent those of the initial state, saddle point and final state from left to right.

suggests high saturation coverage for U surface exposure to a hydrogen environment.

To correlate a given hydrogen chemical potential μ_H with experimental conditions, we have also explored the temperature and pressure dependence of μ_H. Hydrogen behaves similarly to an ideal gas, so μ_H can be described using the following formula:

$$\mu_H = \frac{1}{2}\left[E_{H_2} + \tilde{\mu}_{H_2}(p^0, T) + k_B T \ln\left(\frac{p_{H_2}}{p^0}\right)\right] \qquad (5)$$

where p^0 corresponds to standard pressure and $\tilde{\mu}_{H_2}$ includes the contributions from rotations and vibrations of the hydrogen molecule, as well as the ideal gas entropy at 1 atm. These are listed in thermodynamic tables and allow the determination of $\tilde{\mu}_{H_2}$ [24–26]. Using equation (5), the two-dimensional phase diagram of the temperature and pressure dependence is as shown in figure 3(b).

The dissociation of H_2 molecules on α-U(001) surface has been studied using the climbing NEB method. The 1×1 supercell with three layers of U atoms has been considered. All calculations were performed using eight images along the reaction path. To investigate the energy profiles for H_2 dissociation starting from different initial states, three reaction paths have been considered. The first reaction path corresponds to the dissociation starting from the molecular adsorption configuration of Hor1 on the threefold hollow2 site as described previously, the second one starts from the Hor2 configuration on the hollow2 site H–H bond which differs by being at an angle of 90° to that of the first path, and the third dissociation path starts from the Hor1 configuration on the onefold top site. By considering these three paths, we intend to investigate the influence of the starting orientation of the H–H bond or the located site of H_2 on the dissociation behavior. The dissociated configuration with two H atoms located on the adjacent threefold hollow sites was optimized and taken as a possible final state in all three dissociation processes. The energy profiles for these reactions are depicted in figure 4. Every point on the energy curves (including those

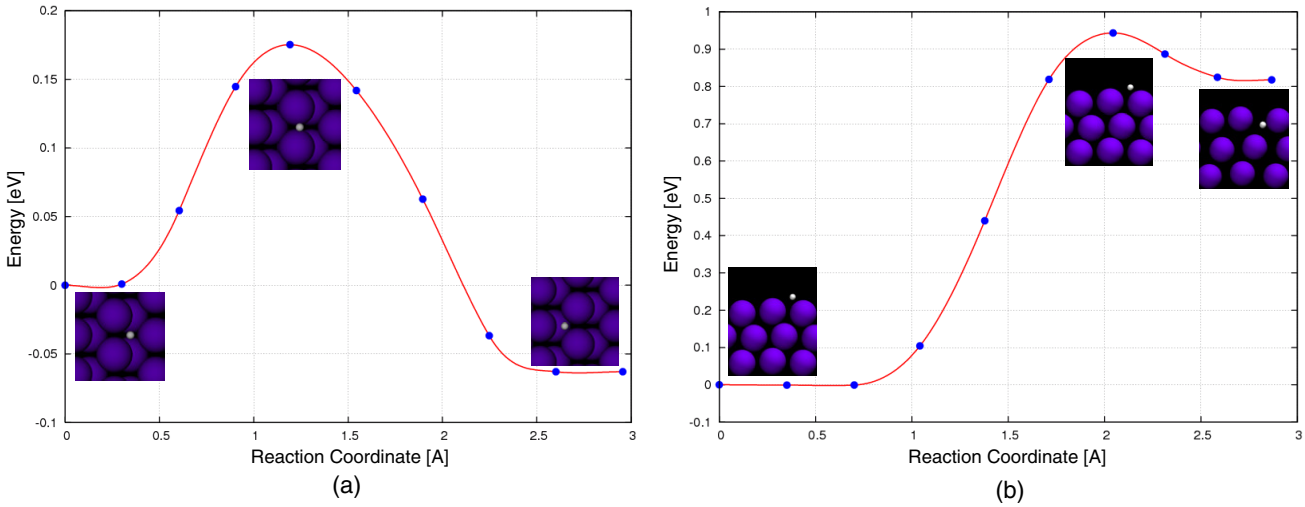

Figure 5. Potential energy surface for diffusion of atomic H (a) between the adjacent hollow1 and hollow2 sites, (b) penetrating the U surface. The inset structures represent those of the initial state, saddle point and final state from left to right.

for the H diffusion) corresponds to an image in sequence from left to right (for images 0–9). The inset structures represent the initial state, the saddle point and the final state from left to right. For the sake of clarity, we have also summarized the representative structural parameters for the initial state, saddle point and final state along different paths in table 3.

For the first dissociation path, the energy barrier which is defined as the activation energy to be supplied at 0 K to proceed to the dissociation process was calculated to be 0.34 eV. Huda and Ray have obtained a barrier of ∼0.2 eV for H_2 dissociation on Pu(111) within the DFT framework [20]. The saddle point was found to locate at image 3, which corresponds to a configuration having a stretched H–H distance of 1.315 Å without any rotation parallel to the surface with respect to the initial state. The titled angle for the H–H bond relative to the surface normal is calculated to be ∼65°, indicating a rotation of ∼10° in the surface perpendicular to the U surface relative to the initial state. One H atom was found to locate nearly at the hollow site as shown in the inset structure. A local minimum (image 6) exists at an H–H distance of 3.216 Å, where H atoms sit nearly on two adjacent hollow2 sites. The activation energy for the formation of the molecule, i.e. the inverse barrier, is determined from the energy difference between this dissociated state and the saddle point to be 1.188 eV. This large energy barrier value for H_2 on the U surface also supports the U surface being easily hydrided in the environment of the atmosphere. A low barrier of 0.116 eV was found to exist for the transformation from the local minimum state to the final state.

Figure 4(b) shows the energy profile of the dissociation process along the second path. It is found that an H_2 molecule quickly reaches the energy maximum at image 1. The reaction barrier was calculated to be 0.13 eV which is 0.21 eV lower than for the dissociation along the first path. This indicates the interesting behavior that H_2 adsorbed on the same threefold site 'prefers' to dissociate from an initial orientation perpendicular rather than parallel to the orientation of the H–H bond in the final state. The geometry investigation

Table 3. The important geometric parameters for the initial state, saddle point and final state along the different dissociation paths. IS, SP and FS represent the initial state, saddle point and final state, respectively.

		R(H–H) (Å)	R(H–U) (Å)		h(H–Surf) (Å)		φ (deg)
Path 1	IS	0.790	2.385	2.454	2.255	2.448	75.8
	SP	1.315	2.173	2.036	1.462	2.012	65.3
Path 2	IS	0.821	2.345	2.345	2.311	2.311	90.0
	SP	0.868	2.279	2.306	1.882	1.924	87.2
Path 3	IS	0.789	2.385	2.394	2.339	2.325	88.9
	SP	0.867	2.275	2.298	1.893	1.933	87.4
	FS	2.314	2.221	2.226	1.361	1.341	89.7

of the saddle point yielded an H–H bond length of 0.868 Å which is only 0.12 Å longer than the optimized bond length of H_2, indicating that the H–H bond of the saddle point along the second dissociation path is not dissociated. The similar phenomenon that one H atom moves close to the hollow site is also observed. Considerable rotation of H_2 parallel to the surface was observed, as illustrated in the inset structure in figure 4(b). Two local minima exist at images 5 and 7 which were found to have much larger H–H distances than the neighboring images. A very small barrier of 0.07 eV was determined for transition between these two configurations.

The result for the third dissociation pathway is illustrated in figure 4(c). It is shown that the reaction barrier for H_2 dissociation starting from the Hor1 configuration on the top site is 0.081 eV, i.e. H_2 is much easier to dissociate from the top rather than the optimized hollow site. The saddle point was found to locate at image 3, for which the H–H distance was calculated to be 0.867 Å, indicating molecular adsorption for the saddle point. It is interesting to find a rotation of the H_2 molecule similar to that for path 2. One H atom is also found to locate close to the threefold site. A local minimum is present at image 7 at an H–H distance of 3.122 Å. On the basis of the analysis of the three dissociation paths, we see that the third dissociation path is most energetically preferred. For

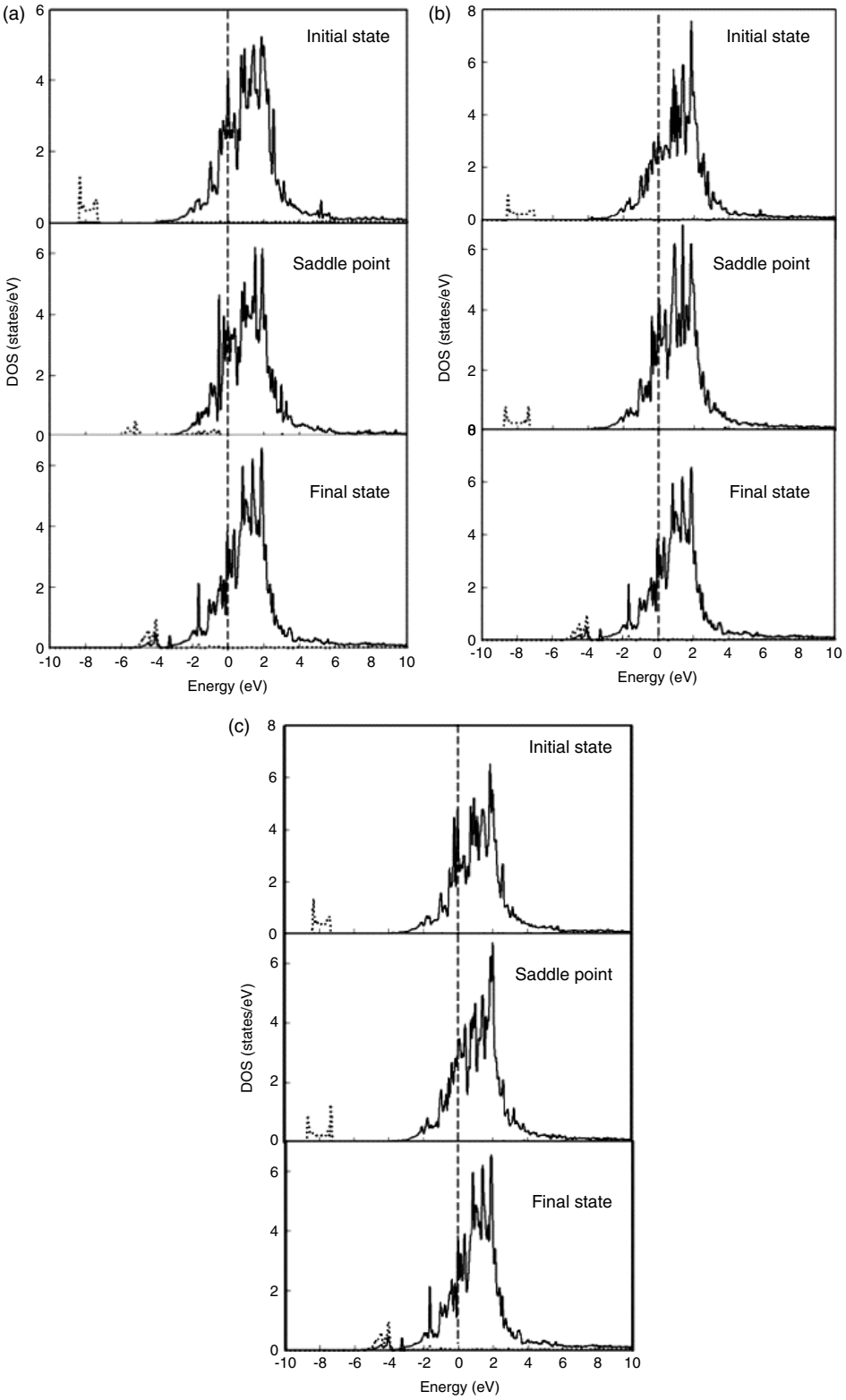

Figure 6. U 5f (solid line) and H_2 1s (dotted line) DOS for the initial state, saddle point and final state for dissociation process starting from (a) Hor1 on the hollow2 site, (b) Hor2 on the hollow2 site and (c) Hor1 on the top site.

all dissociation paths considered, we observed that the saddle points correspond to configurations with one H atom located close to the threefold hollow site.

To obtain the MEP for the atomic H diffusion following molecular dissociation, we have performed a climbing NEB calculation for the H atom diffusion processes. Two situations were considered. The first is an on-surface diffusion of H between the most stable threefold sites hollow1 and hollow2. The second is the penetrating motion of H, i.e. the H atom diffuses from the most stable on-surface site hollow2 to the

Table 4. Charge distribution of the dissociated adsorption structure of α-U(001) (1 × 1)–2H. A negative value represents charge gain, whereas a positive value corresponds to charge loss.

	H atom		Layer 1		Layer 2		Layer 3	
Charge	−0.454	−0.443	0.593	0.337	0.004	0.007	−0.019	−0.024

stable subsurface site sub2 which is direct below the hollow2 site. The minimum energy paths corresponding to these processes are presented in figures 5(a) and (b).

In the case of the on-surface diffusion motion between two threefold sites, it can be seen in figure 5(a) that the curve has a maximum at image 4 which corresponds to a configuration with the H atom residing very close to the short-bridge site. Thus, the short-bridge site is a saddle point for atomic diffusion of H between two adjacent threefold sites. The barrier for this diffusion path is determined as 0.175 eV. This low energy barrier clearly indicates fast diffusion even at room temperature.

Figure 5(b) shows the PES describing the motion from the on-surface threefold site to the subsurface site between the first and second U layers (i.e. the interstitial position). It is indicated that the energy surface is quite flat before it reaches image 3, which corresponds to a configuration having a height of 1.16 Å for the H atom (that for the initial state is 1.397 Å) relative to the U surface. The energy climbs very sharply until it meets a maximum at image 6. This saddle point corresponds to a configuration in which the H atom locates almost in the plane of the top substrate layer. The activation energy for H penetrating into the metal is estimated to be ∼0.94 eV. With this high barrier, it is not easy for hydrogen to penetrate into the bulk U.

Understanding the signature role of the 5f electrons in bonding and localization is one of the key issues for actinide surfaces, that has gained much attention. Thus, we have studied the electronic structure of the H–U system along the dissociation paths considered. Figures 6(a)–(c) show the projected densities of states (PDOSs) for a number of configurations along the MEPs: initial state, saddle point, and the final state. In all the DOS plots the Fermi levels are scaled to zero.

For all the three dissociation paths considered, it is shown that there is no overlap between the H_2 molecular orbitals and the 5f orbital of the U surface for the initial state, i.e. the molecular adsorption configuration for which the hydrogen molecule is still far from the metal surface (about 1 Å higher than for atomic adsorption). Hence, the bonding between the hydrogen molecule and the uranium surface is very weak, possibly of van der Waals type. A similar conclusion has also been drawn for H_2 adsorption on the Pu(111) surface [20]. The saddle points for different dissociation paths are somewhat different in geometry as described previously. For the second and third dissociation paths where H_2 molecules are not dissociated at the saddle point, there is no overlap between the H_2 orbitals and U 5f states, similar to the initial state case. For the first dissociation path, it is observed that some of the 1s states have extended toward the Fermi level and mixed with U 5f states. This is attributed to one of the H atoms which has shorter bond length with the U atom. For the final state (the same for all paths), the corresponding DOS plots of the third figure in figure 6 show that there exists strong hybridization of U 5f and H_2 1s orbitals, and hence the contribution of the covalent part in the H–U bonding exists in the dissociated adsorption.

To investigate the charge transfer for the dissociated adsorption, we have calculated the Bader charges [27] of the final state as listed in table 4. All the charge values discussed are relative to a bare relaxed surface. We found that the charge distribution patterns of the α-U(001) surface have changed significantly upon H adsorption. The charges located at the H adatoms are very large (∼0.4|e|), indicating significant charge transfer from the substrate to adsorbates. Thus, the ionic part of the H–U bonding plays a significant role in the dissociative adsorption, along with the covalent part due to U 5f and H 1s hybridization. Similar results have also been reported for dissociation adsorption of H_2 on the Pu(111) surface [20].

4. Conclusion

In the current work, hydrogen adsorption, dissociation, and diffusion on the α-U(001) surface has been studied within the framework of density functional theory. Two adsorption coverages, 0.25 and 0.5 ML, were considered. It is found that H_2 physisorbs when approaching with the H–H bond perpendicular to the U surface. Weak molecular chemisorption was observed for H_2 approaching with its molecular axis parallel to the surface. At both coverages, the final adsorption configurations of H_2 on the hollow sites were found to be similar to that for the top site. H_2 dissociation starting from the top site was found to be more favorable than those from the optimized hollow site adsorption configurations in which H_2 is still somewhat deviated from the top site. A low dissociation barrier of 0.081 eV was determined for H_2 dissociated from the top site with the H atoms falling into the two adjacent threefold hollow sites. For all dissociation paths considered, we observed that the saddle points correspond to configurations with one H atom located close to the threefold hollow site. The analysis of the density of states along the dissociation paths shows that the hybridization of U 5f and H 1s states only occurs when the H_2 molecule is dissociated. The H–U bond in the dissociated adsorption configurations is partly ionic and partly covalent.

Acknowledgments

This research was supported by the National Science Foundation of China (10647111), the program for W040632 and JX05019. One of the authors (Fei Gao) was supported by the Division of Materials Sciences and Engineering, Office of Basic Energy Sciences, US Department of Energy, under Contract DE-AC05-76RL01830.

References

[1] Balasubramanian K, Siekhaus W J and McLean W 2003 *Plutonium Futures—The Science* vol 673, p 125
[2] Bloch J and Mintz M H 1981 *J. Less-Common Met.* **81** 301
[3] Condon J B 1975 *J. Phys. Chem.* **79** 42
[4] Condon J B and Larson E A 1973 *J. Chem. Phys.* **59** 855
[5] DeMint A L and Leckey J H 2000 *J. Nucl. Mater.* **281** 208
[6] Kirkpatrick J R 1981 *J. Phys. Chem.* **85** 3444
[7] Powell G L, Harper W L and Kirkpatrick J R 1991 *J. Less-Common Met.* **172** 116
[8] Dholabhai P P and Ray A K 2007 *J. Alloys Compounds* **444** 356
[9] Huda M N and Ray A K 2005 *Int. J. Quantum Chem.* **102** 98
[10] Senanayake S D, Soon A, Kohlmeyer A, Sohnel T and Idriss H 2005 *J. Vac. Sci. Technol.* A **23** 1078
[11] Kresse G and Fürthmuller J 1996 *Phys. Rev.* B **54** 11169
[12] Blochl P E 1994 *Phys. Rev.* B **50** 17953
[13] Kresse G and Joubert D 1999 *Phys. Rev.* B **59** 1758
[14] Perdew J P, Chevary J A, Vosko S H, Jackson K A, Pederson M R, Singh D J and Fiolhais C 1992 *Phys. Rev.* B **46** 6671
[15] Nie J L, Xiao H Y, Zu X T and Gao F 2008 *J. Alloys Compounds* at press
[16] Mills G, Jonsson H and Schenter G K 1995 *Surf. Sci.* **324** 305
[17] Jonsson H, Mills G and Jakobsen K W 1998 *Classical and Quantum Dynamics in Condensed Phase Simulations* ed B J Berne, G Ciccotti and D F Coker (Singapore: World Scientific)
[18] Henkelman G, Uberuaga B P and Jonsson H 2000 *J. Chem. Phys.* **113** 9901
[19] Henkelman G and Jonsson H 2000 *J. Chem. Phys.* **113** 9978
[20] Huda M N and Ray A K 2005 *Phys. Rev.* B **72** 085101
[21] Balooch M and Hamza A V 1996 *J. Nucl. Mater.* **230** 259
[22] Cakmak M, Srivastava G P and Ellialtioglu S 2003 *Phys. Rev.* B **67** 205314
[23] Qian G X, Martin R M and Chadi D J 1988 *Phys. Rev.* B **38** 7649
[24] Reuter K and Scheffler M 2002 *Phys. Rev.* B **65** 035406
[25] Soon A, Todorova M, Delley B and Stampfl C 2006 *Phys. Rev.* B **73** 165424
[26] Stull D R and Prophet H 1971 *JANAF Thermochemical Tables* (Washington, DC: US National Bureau of Standards)
[27] Bader R 1990 *Atoms in Molecules: a Quantum Theory* (New York: Oxford University Press)